Electronic Supplementary Information (ESI)

Ionic covalent organic framework for selective detection and adsorption of TcO_4^-/ReO_4^-

Xiao-Rong Chen[a], Cheng-Rong Zhang[a], Xin Liu[a], Ru-Ping Liang[a,*] and Jian-Ding Qiu[a,b,*]

[a]College of Chemistry, Nanchang University, Nanchang 330031, China

[b]State Key Laboratory of Nuclear Resources and Environment, East China University of Technology, Nanchang 330013, China

*Corresponding authors. Tel/Fax: +86-791-83969518. E-mail: rpliang@ncu.edu.cn; jdqiu@ncu.edu.cn.

EXPERIMENT SECTION

Materials.

The Re ICP standard solution (1000 mg/L in 2% nitric acid) was purchased from Henan Wanjia R&D Center Co., Ltd. 4,4',4",4"'-([9,9'-bicarbazole]-3,3',6,6'-tetrayl)tetraaniline (BTTA) and 1,1-bis(2,4-dinitrophenyl)-4,4-bipyridinium dichloride (BDNP) were purchased from Jilin Chinese Academy of Sciences-Yanshen Technology Co., Ltd. Sodium Perrhenate ($NaReO_4$) was purchased from Energy Chemical Technology (Shanghai) Co., Ltd. Ethanol (EtOH), tetrahydrofuran (THF), N,N-dimethylformamide (DMF) and other nitrate salts were purchased from Sinopharm Chemical Reagent Co., Ltd. Ultrapure water was prepared from the Millipore system (18.25 MΩ cm). All reagents were used without further purification, and all the experiments were conducted at room temperature.

Instruments.

Fourier-transform infrared (FT-IR) spectra were recorded with a Bruker TENSOR 27 instrument. Powder X-ray diffraction (PXRD) data of the nanomaterials were collected on a Bruker AXS D8 Advance A25 Powder X-ray diffractometer (40 kV, 40 mA) using Cu Kα (λ=1.5406 Å) radiation. The fluorescence (FL) spectra were recorded on a FL spectrophotometer (F-7000, Hitachi). Time-resolved spectra were recorded with a FLS1000 instrument. X-ray photoelectron spectroscopy (XPS) spectra were performed on a Thermo VG Multilab 2000X with Al Kα irradiation. The radiation stability of BTTA-BDNP was investigated in a GAMMATOR M-38-2 (USA) irradiator with a 60Co source (γ-ray). Solid-state NMR experiments were performed on a Bruker WB Advance II 600 MHz NMR spectrometer. The ^{13}C CP/MAS NMR spectra were recorded with a 4-mm double-resonance MAS probe and with a sample spinning rate of 10.0 kHz; a contact time of 2 ms (ramp 100) and a pulse delay of 3 s were applied. The nitrogen adsorption and desorption isotherms were measured at 77 K using a Micromeritics ASAP 2020M system. The samples were outgassed at 120 °C for 8 h before the measurements. Surface areas were calculated from the adsorption data using Brunauer-Emmett-Teller (BET) methods. The pore-size-distribution curves were obtained via the non-local density functional

theory (NLDFT) method. The thermal properties of the nanomaterials were evaluated using a STA PT1600 Linseis thermogravimetric analysis (TGA) instrument over the temperature range of 30 to 800 °C under nitrogen atmosphere with a heating rate of 10 °C/min. Metal ions concentrations were determined using an iCAP Q inductively coupled plasma mass spectrometry (ICP-MS, Thermo Fisher Scientific, USA).

Synthesis of BTTA-BDNP COF.

BTTA-BDNP was synthesized via the Zincke reaction of 4,4',4",4"'-([9,9'-bicarbazole]-3,3',6,6'-tetrayl)tetraaniline (BTTA) and 1,1-bis(2,4-dinitrophenyl)-4,4-bipyridinium dichloride (BDNP). A mixture of BTTA (25.78 mg, 37 μmol) and BDNP (41.54 mg, 74 μmol) were added to the microwave reaction vessel. Then, 12 mL of ethanol (EtOH) and 3 mL of ultra-pure water were added to the microwave reaction vessel. The mixture was sonicated for 10 min, reacted at 90 °C under microwave irradiation for 2 h. The solid produced in the reaction was collected by centrifugation. The obtained solid was washed several times with ethanol and ultra-pure water, dried in a vacuum oven at 60 °C for 12 h to obtain a reddish-brown powder.

Detection Experiment.

The BTTA-BDNP solution (0.25 mg/mL) was prepared by dissolving the BTTA-BDNP in deionized DMF. The ionic reserve fluids (1 mM) were prepared by dissolving the corresponding sodium salts or nitrate salts of ReO_4^-, Na^+, Cl^-, Br^-, Co^{2+}, ClO_4^-, SO_4^{2-}, PO_4^{3-}, I^-, NO_3^-, CO_3^{2-}, F^-, K^+, Ca^{2+}, and Fe^{3+} in ultrapure water. For ReO_4^- sensing, the various concentrations of ReO_4^- (20 μL) were added to the BTTA-BDNP suspension (40 μL), then DMF (440 μL) was added to the solution to dilute the volume to 500 μL. To further investigate the effect of other interfering ions on ReO_4^- detection, the solution of interfering ions or mixed ion (20 μL, 400 μM) were added to BTTA-BDNP COF suspension. The fluorescence spectra were measured from 420 to

650 nm employing the excitation of 400 nm. Detection limit = 3σ / K, σ is the standard deviation of the fluorescence intensity of the blank solution and K corresponds to slope of linear equation.

Recyclability.

Regenerate BTTA-BDNP by treating with equal volume of NaCl (3 M) solution and shaking for 24 hours. The resulting suspension was filtered and washed with ultrapure water several times. After vacuum drying, the resulting material was used in another detection experiment.

Sorption experiment

Optimization of adsorption pH. 5 mg adsorbent was added to 10 mL 28 ppm ReO_4^- aqueous solution with varying pH from 2 to 12. The solution pH was adjusted by adding NaOH and HNO_3. The mixture was shaken at 200 rpm for 24 hours, and separated with a 0.22 μm nylon membrane filter to obtain a clear liquid for ICP analysis.

Sorption isotherm study. The adsorption isotherms study of BTTA-BDNP was conducted by adding 10 mg of adsorbent into 20 mL aqueous solutions of varying the initial concentrations of ReO_4^- (*ca.* 25-1000 mg L^{-1}), then stirred overnight to achieve equilibrium. The suspension was separated with a 0.22 μm nylon membrane filter for ICP-MS analysis. The adsorption capacity was calculated based on equation (1).

$$q_e = \frac{(C_0 - C_e)V}{m} \quad (1)$$

where q_e (mg g^{-1}) is the equilibrium adsorption capacity, C_0 (mg L^{-1}) and C_e (mg L^{-1}) is the initial concentration and equilibrium concentration of ReO_4^-, respectively. m (mg) is the mass of the adsorbent and V (L) is the volume of the solution.

The Langmuir isotherm is based on the assumption that the adsorbent can only be adsorbed in a single layer on the adsorbent. The linear fitting of the Langmuir isotherm model is expressed by equation (2).

$$\frac{C_e}{q_e} = \frac{1}{q_m k_L} + \frac{C_e}{q_m} \quad (2)$$

where q_m (mg g^{-1}) is the maximum sorption capacity, k_L is a constant indirectly related to sorption capacity and energy of sorption (L mg^{-1}), which characterizes the affinity of the adsorbate with the adsorbent.

The Freundlich model is an empirical equation based on sorption on a heterogeneous surface. The linear fitting of the Freundlich isotherm model is expressed by equation (3).

$$\ln q_e = \ln k_F + \frac{1}{n} \ln C_e \quad (3)$$

where k_F and n are the Freundlich constants related to the sorption capacity and the sorption intensity, respectively.

Sorption kinetics study. The sorption kinetics experiments were carried out under the conditions of pH 7 and solid-liquid ratio 0.5 g L^{-1}. 10 mg of BTTA-BDNP was added into 20 mL aqueous solutions of the initial concentrations of ReO_4^- (28 $mg \cdot L^{-1}$). Under magnetic stirring, the resulting mixture was stirred for a desired contact time (1 min, 3 min, 6 min, 20 min, 40 min and 60 min), then take 1 mL samples and using 0.22 um nylon membrane filter for ICP-MS detection. The removal rate (RE) was calculated based on equation (4). The distribution coefficient (K_d) of BTTA-BDNP toward ReO_4^- was calculated based on equation (5).

$$\mathrm{RE} = \frac{(C_0 - C_t)}{C_0} \times 100\% \quad (4)$$

$$\mathrm{K}_d = \frac{V(C_0 - C_e)}{mC_e} \quad (5)$$

where C_t is the concentration of ReO_4^- at time t.

Removal rate in simulated wastes. According to reported research, we prepared the simulated Hanford LAW Melter Recycle solution. The experiment was conducted as follows. 5 mg, 25 mg adsorbent was added to 5 mL of the above simulated solution, respectively. The mixture was shaken at 150 rpm for 24 hours, and separated with a 0.22 μm nylon membrane filter to obtain a clear liquid for ICP analysis.

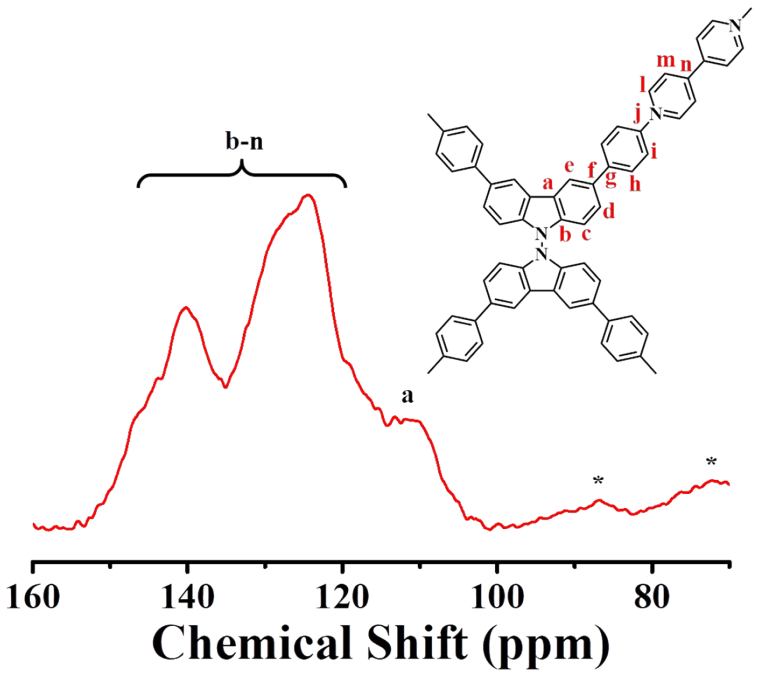

Fig. S1. Solid-state ^{13}C CP/MAS NMR spectrum of BTTA-BDNP.

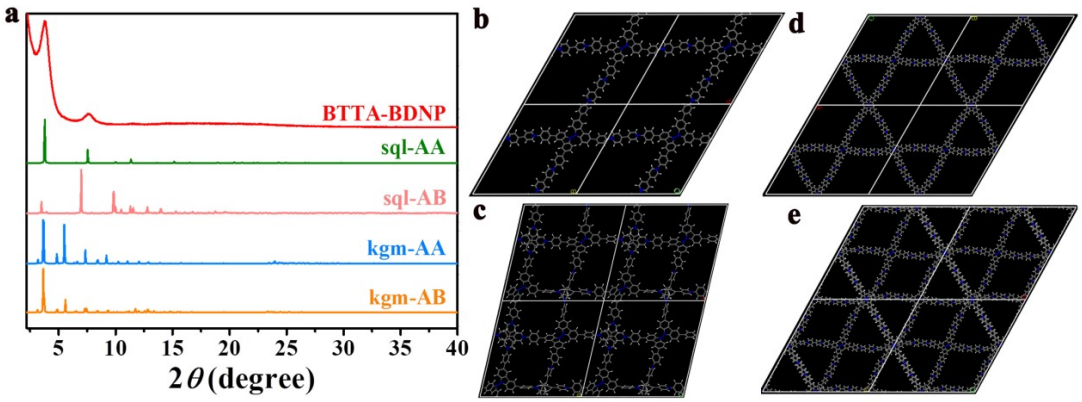

Fig. S2. (a) Experimental PXRD patterns of BTTA-BDNP (red), simulated profiles for monoclinic sql-AA model (green), sql-AB model (pink), kgm-AA model (bule) and kgm-AB model (orange). (b) sql-AA model and (c) sql-AB model crystal lattice packing of BTTA-BDNP. (d) kgm-AA model and (e) kgm-AB model crystal lattice packing of BTTA-BDNP.

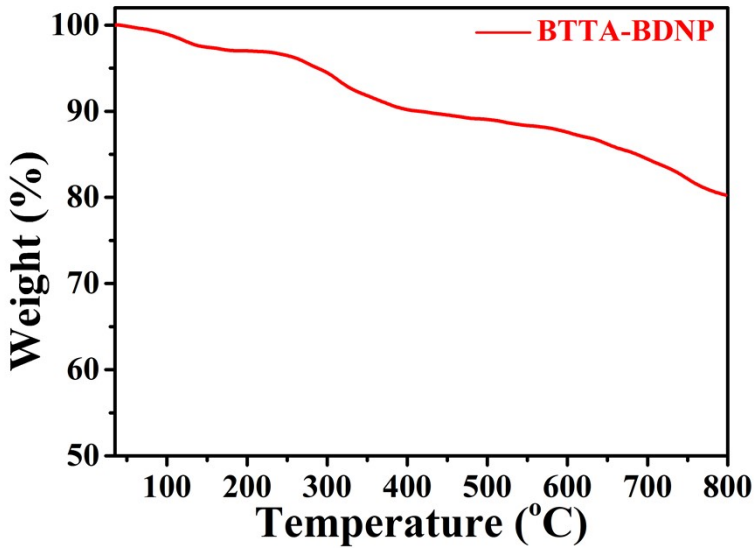

Fig. S3. TGA curve of BTTA-BDNP under N_2 atmosphere.

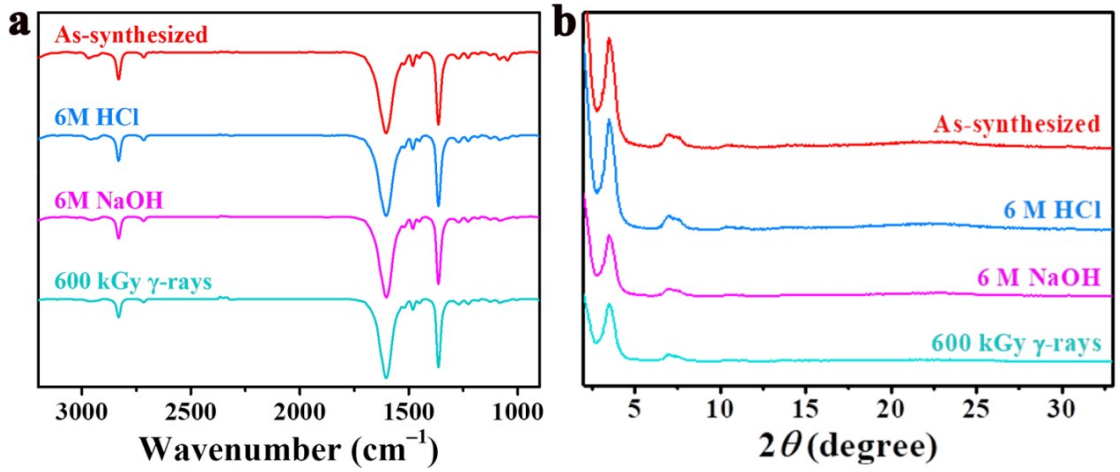

Fig. S4. (a) FT-IR spectra and (b) PXRD patterns of BTTA-BDNP before and after treatment with 600 kGy γ-ray irradiation, 6 M NaOH, and 6 M HCl for 12 h.

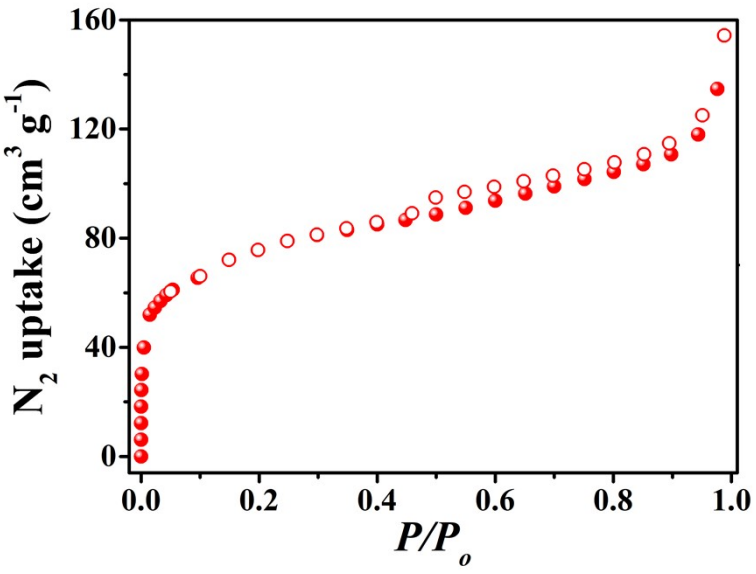

Fig. S5. Nitrogen-sorption isotherm curves measured at 77 K for BTTA-BDNP.

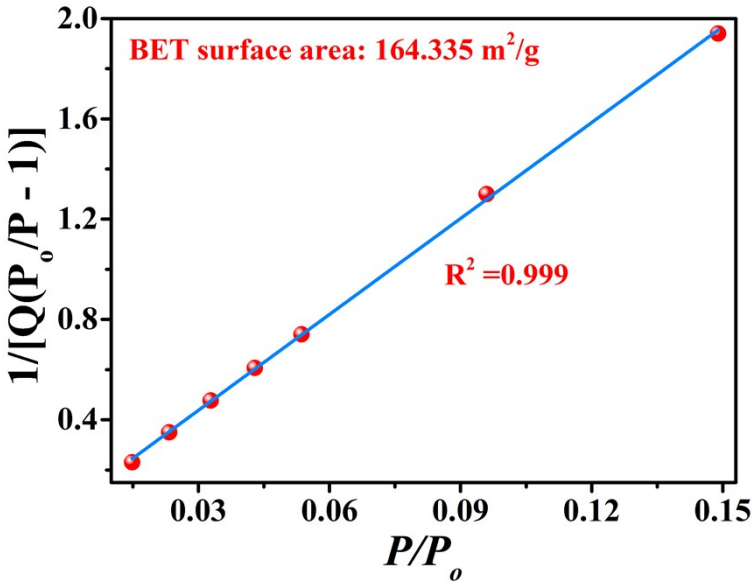

Fig. S6. BET surface area plots of BTTA-BDNP.

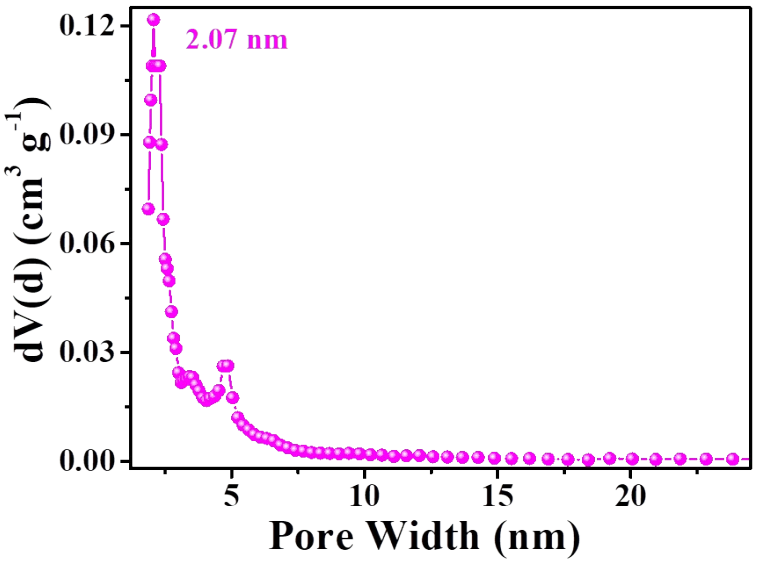

Fig. S7. Pore-size distribution profiles of BTTA-BDNP.

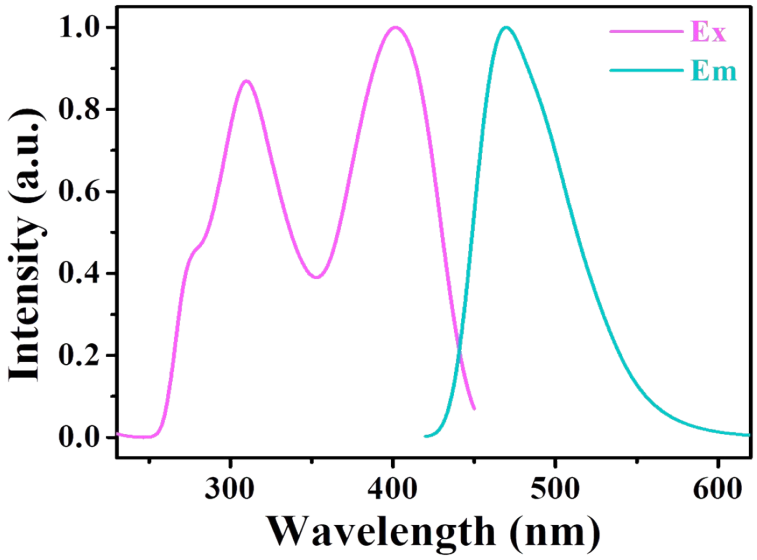

Fig. S8. Normalized fluorescence excitation and emission spectra of BTTA-BDNP dispersed in DMF.

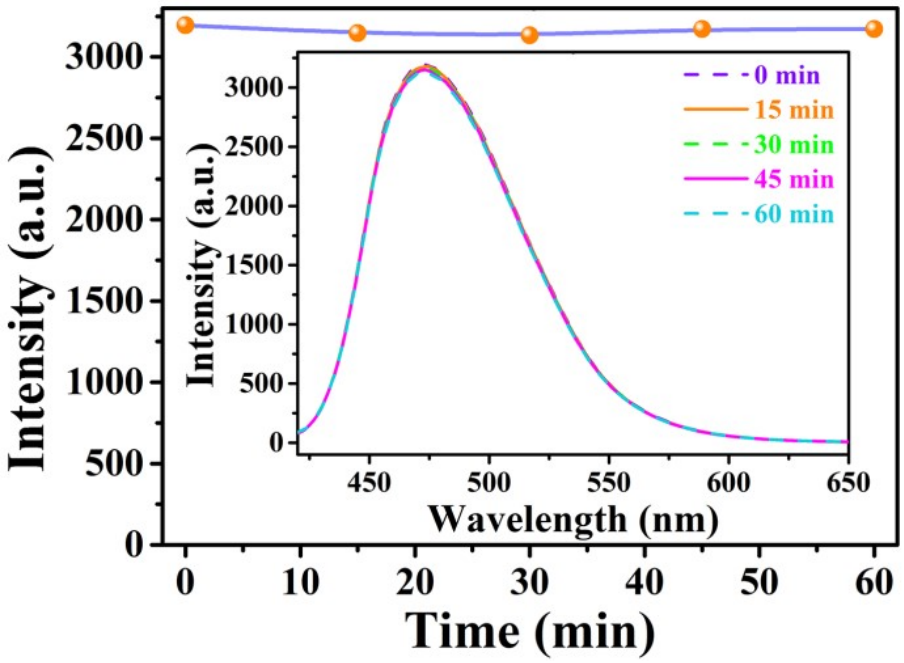

Fig. S9. Time-dependent fluorescence intensity of BTTA-BDNP (dispersed in DMF) tested within 60 minutes.

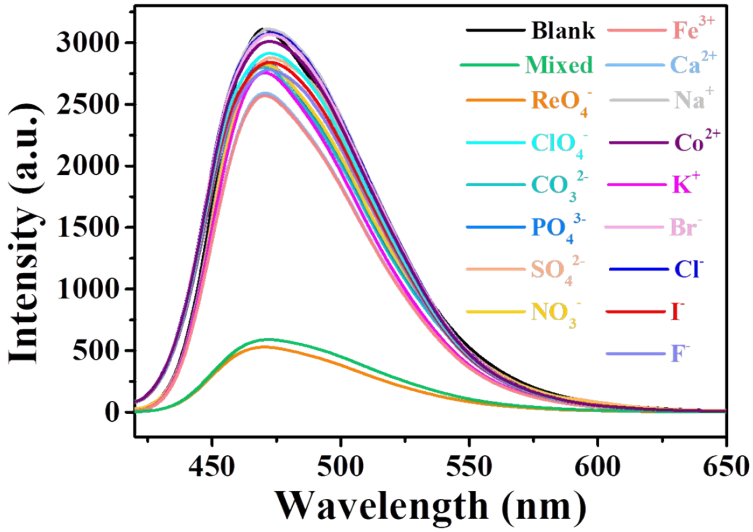

Fig. S10. Fluorescence intensity of the BTTA-BDNP COF at 470 nm in the presence of 500 μM of interfering ions or 100 μM of ReO_4^-.

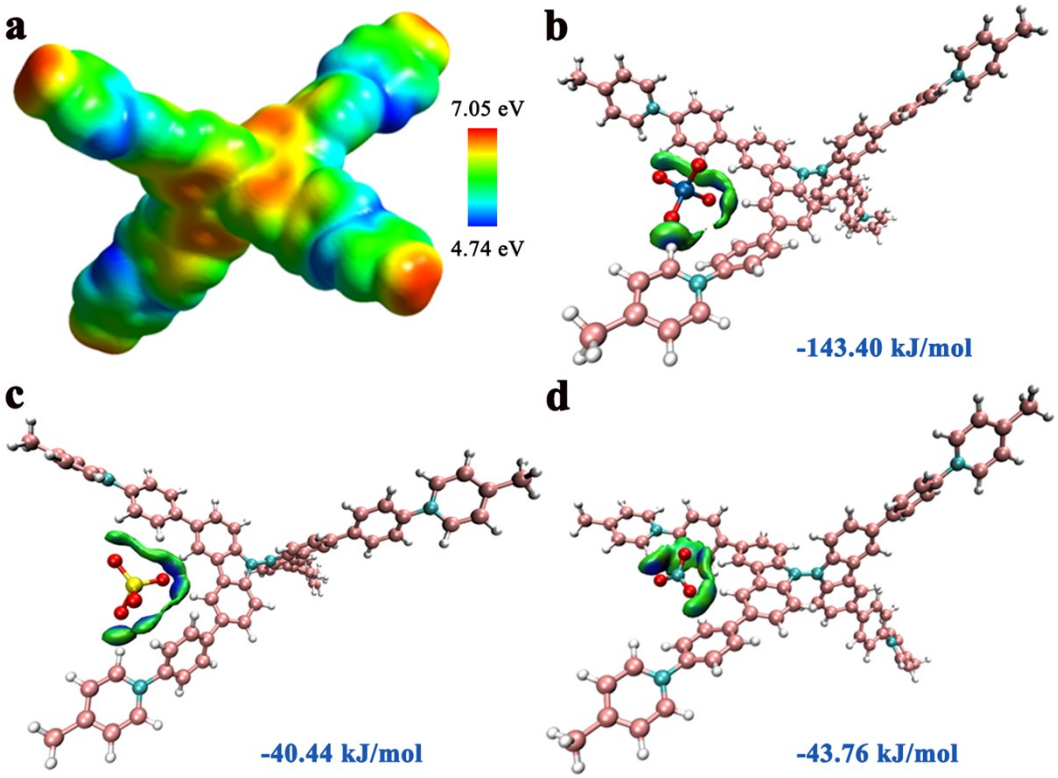

Fig. S11. (a) ESP map of the BTTA-BDNP fragment. (b) IGM analysis and binding energies of (b) BTTA-BDNP-ReO_4^-, (c) BTTA-BDNP-SO_4^{2-} and (d) BTTA-BDNP-NO_3^-.

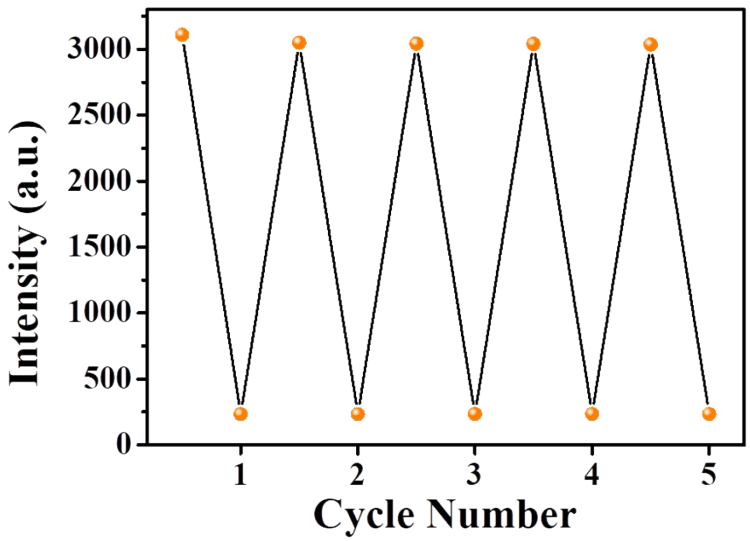

Fig. S12. Recycle use of BTTA-BDNP for selective detection of ReO_4^-.

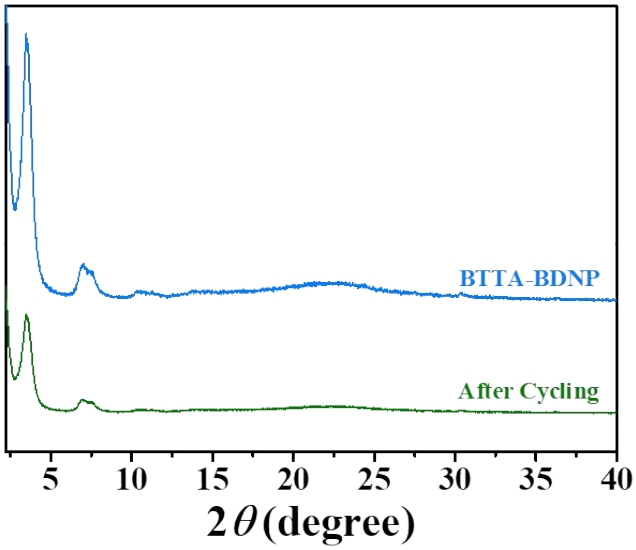

Fig. S13. The PXRD patterns of BTTA-BDNP before and after recycling test.

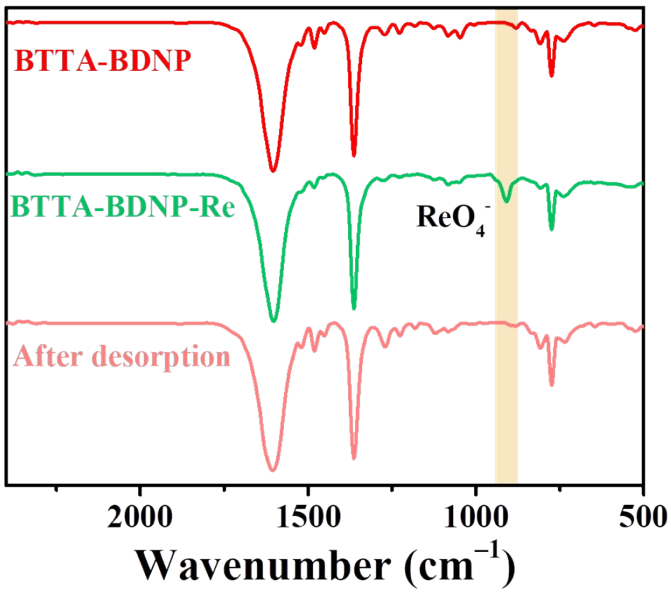

Fig. S14. FT-IR spectra of BTTA-BDNP before and after adsorption as well as after desorption.

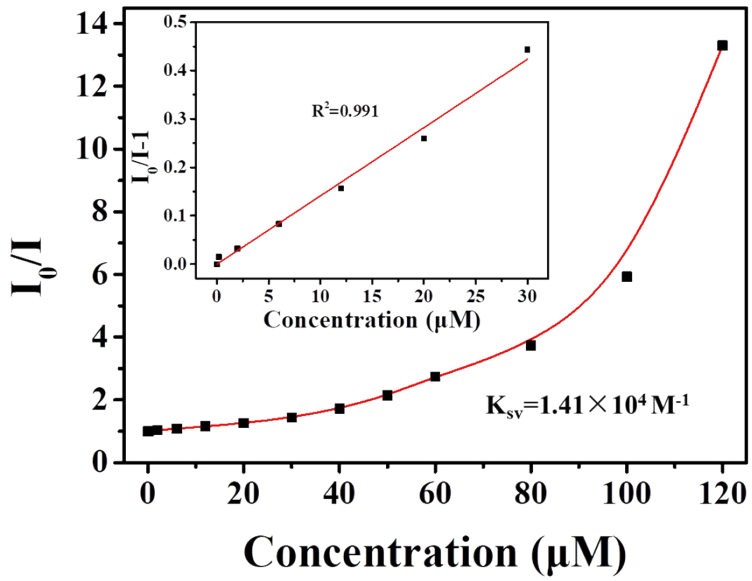

Fig. S15. Stern-Volmer plot of BTTA-BDNP for detecting ReO_4^-. Inset: Determination of K_{sv} value for BTTA-BDNP for detecting ReO_4^-.

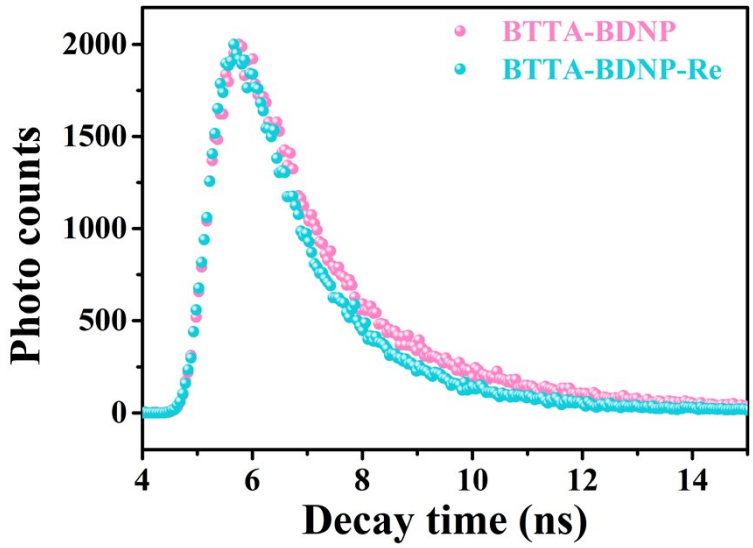

Fig. S16. Fluorescence decay profiles of BTTA-BDNP obtained by treatment without and with ReO_4^-.

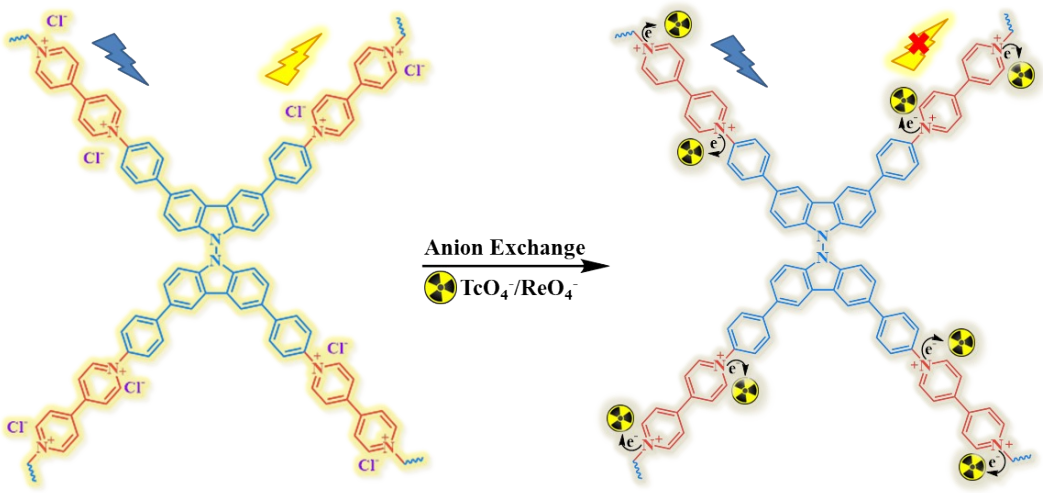

Fig. 17. Fluorescence enhancement mechanism.

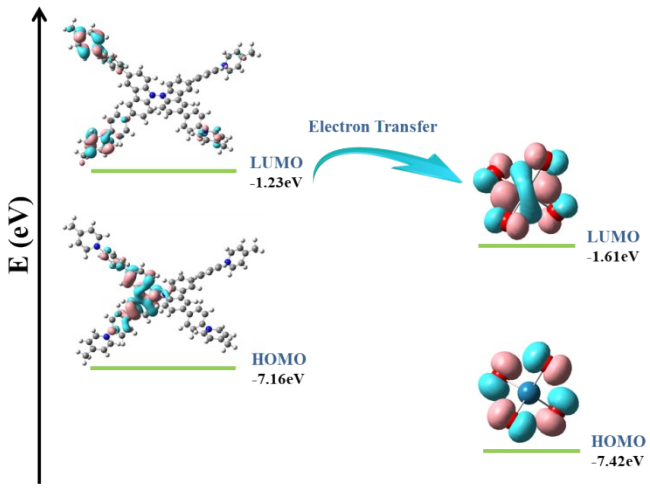

Fig. S18. Highest occupied molecular orbital (HOMO) and lowest unoccupied molecular orbital (LUMO) energy levels of BTTA-BDNP, and ReO_4^- computed by DFT.

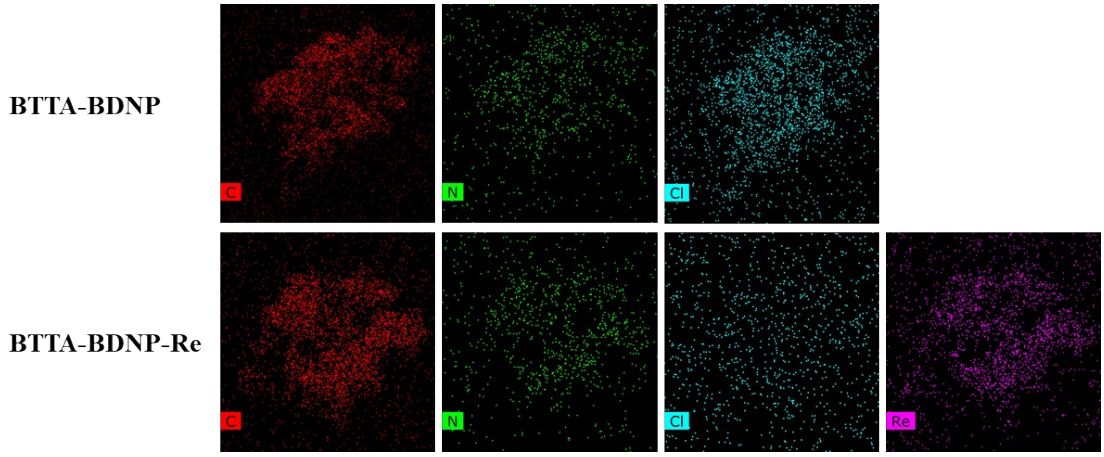

Fig. S19. SEM-EDS maps of BTTA-BDNP and BTTA-BDNP-Re.

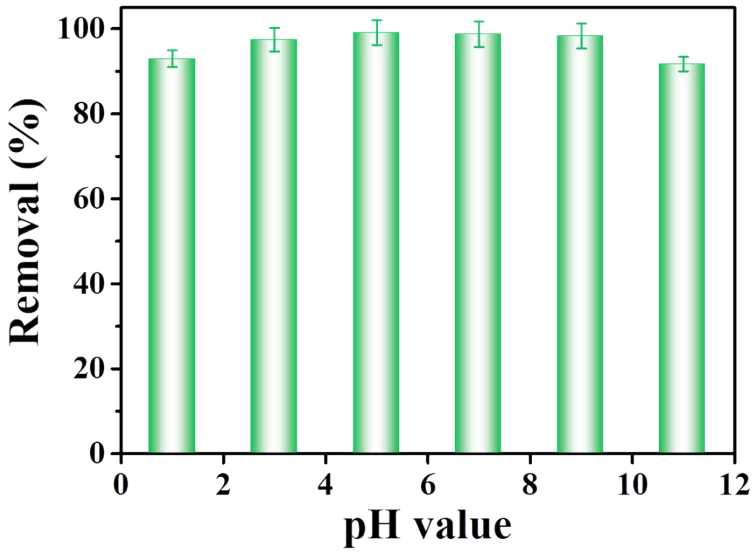

Fig. S20. Influence of pH for ReO_4^- capture employing BTTA-BDNP.

Table S1. Fractional atomic coordinates for the sql-AA stacking unit cell of BTTA-BDNP.

Space group: P 1 (1) - triclinic ***a=27.1347 Å, b = 27.2678 Å, c = 4.1703 Å*** ***α = β = 90°, γ = 120°***							
Atom	***x***	***y***	***z***	**Atom**	***x***	***y***	***z***
C1	0.6428	0.30412	0.70932	C42	0.42034	0.34303	-0.26594
C2	0.60073	0.27621	0.90265	N43	0.28463	0.34635	-0.39181
C3	0.5971	0.2278	1.0267	C44	0.25575	0.30585	-0.58361
C4	0.63526	0.20817	0.95613	C45	0.20959	0.30378	-0.71995
C5	0.67798	0.23804	0.76142	C46	0.19116	0.34271	-0.65692
C6	0.68056	0.28579	0.64232	C47	0.22096	0.38347	-0.45669
C7	0.63053	0.15664	1.08482	C48	0.26776	0.38504	-0.32935
C8	0.63367	0.11498	0.92971	C49	0.7038	0.36643	0.40288
C9	0.62981	0.06656	1.05016	C50	0.73289	0.41128	0.22347
C10	0.62301	0.05896	1.32847	C51	0.78004	0.41472	0.08658
C11	0.62007	0.10081	1.48389	C52	0.79757	0.37377	0.1317
C12	0.62354	0.14911	1.36293	C53	0.76657	0.32854	0.31403
C13	0.63616	0.43265	0.71396	C54	0.72002	0.32609	0.44529
C14	0.67848	0.46096	0.90583	C55	0.84805	0.37826	-0.00968
C15	0.68052	0.50794	1.03721	C56	0.88607	0.36544	0.12443
C16	0.64085	0.5261	0.97361	C57	0.93255	0.36785	-0.01033
C17	0.59828	0.4962	0.77849	C58	0.94227	0.3838	-0.28023
C18	0.59693	0.44951	0.65378	C59	0.90516	0.39764	-0.41392
C19	0.64348	0.57573	1.1124	C60	0.85827	0.39465	-0.28031
C20	0.63949	0.61798	0.9663	N61	0.64669	0.94718	2.18641
C21	0.64085	0.66431	1.09706	C62	0.59624	0.90181	2.1028
C22	0.6457	0.66911	1.37717	C63	0.5954	0.85595	1.97008
C23	0.64992	0.6268	1.52296	C64	0.64687	0.85673	1.91746
C24	0.64918	0.58078	1.39167	C65	0.6983	0.90427	2.00165
N25	0.64617	0.71653	1.51265	C66	0.69731	0.94896	2.13757
C26	0.68482	0.74456	1.71245	N67	0.04856	0.3375	-1.06464
C27	0.68563	0.79029	1.84701	C68	0.09035	0.38786	-0.95994
C28	0.64682	0.80823	1.77626	C69	0.13738	0.39054	-0.82936
C29	0.60769	0.77913	1.56995	C70	0.14138	0.34088	-0.79828
C30	0.6079	0.73335	1.44122	C71	0.0972	0.28943	-0.9047
C31	0.57546	0.37009	0.40734	C72	0.05151	0.28874	-1.03914
C32	0.54686	0.32541	0.22657	N73	0.62455	0.38319	0.56424
C33	0.49871	0.32081	0.09451	N74	0.65592	0.35483	0.56632
C34	0.47961	0.36027	0.14678	H75	0.57195	0.29149	0.95759
C35	0.50989	0.4052	0.33121	H76	0.56429	0.20536	1.17589
C36	0.55763	0.40901	0.45666	H77	0.70866	0.22503	0.70838
C37	0.42845	0.35476	0.00921	H78	0.63866	0.11968	0.71476
C38	0.38788	0.36228	0.15172	H79	0.63184	0.03477	0.9264
C39	0.34051	0.35884	0.02133	H80	0.61605	0.09654	1.69934
C40	0.33284	0.34835	-0.25543	H81	0.62207	0.18124	1.48679
C41	0.37327	0.3402	-0.39714	H82	0.70861	0.44698	0.95438

H83	0.71318	0.53044	1.18693	H103	0.2906	0.41789	-0.18062
H84	0.56668	0.50826	0.72959	H104	0.71983	0.44271	0.19128
H85	0.63584	0.61536	0.75039	H105	0.80336	0.44985	-0.05094
H86	0.63848	0.6967	0.97941	H106	0.77803	0.29603	0.35076
H87	0.65286	0.62896	1.73907	H107	0.88014	0.3539	0.33417
H88	0.65176	0.54838	1.50859	H108	0.96129	0.35769	0.09579
H89	0.71572	0.732	1.76865	H109	0.91207	0.40969	-0.62284
H90	0.71606	0.81088	2.00753	H110	0.82936	0.40401	-0.38995
H91	0.5774	0.79188	1.50632	H111	0.5561	0.90046	2.14236
H92	0.57673	0.71112	1.28487	H112	0.55466	0.81976	1.91332
H93	0.56114	0.29509	0.18886	H113	0.73909	0.90732	1.9608
H94	0.47588	0.28608	-0.04556	H114	0.73734	0.98538	2.20126
H95	0.497	0.43647	0.37334	H115	0.08804	0.4266	-0.98084
H96	0.39259	0.37037	0.36505	H116	0.17065	0.43165	-0.75784
H97	0.30958	0.36403	0.13747	H117	0.09719	0.24961	-0.88274
H98	0.36895	0.33254	-0.61056	H118	0.01798	0.24867	-1.12019
H99	0.45114	0.33739	-0.38086	Cl119	0.29941	0.30452	-0.26618
H100	0.26798	0.27434	-0.63222	Cl120	0.68838	0.69531	1.51265
H101	0.18911	0.27203	-0.8752	Cl121	0.58818	0.9416	2.18641
H102	0.20819	0.41383	-0.39504	Cl122	0.04587	0.39203	-1.06464

Table S2. Fractional atomic coordinates for the sql-AB stacking unit cell of BTTA-BDNP.

Space group: P 1 (1) - triclinic ***a=26.9735 Å, b = 27.8868 Å, c = 6.4092 Å*** ***α = β = 90°, γ = 103.2005°***							
Atom	***x***	***y***	***z***	**Atom**	***x***	***y***	***z***
C1	1.12727	-0.22619	0.16976	C20	1.04927	0.02751	0.7228
C2	1.08079	-0.25174	0.25073	C21	1.04843	0.07727	0.72734
C3	1.07286	-0.30301	0.27283	C22	1.09383	0.11311	0.70317
C4	1.11122	-0.32769	0.21392	C23	1.14038	0.09902	0.69759
C5	1.1577	-0.30078	0.12996	C24	1.14125	0.04941	0.68972
C6	1.16461	-0.25007	0.11142	N25	1.0925	0.16266	0.65421
C7	1.10444	-0.38073	0.25387	C26	1.07362	0.17279	0.46521
C8	1.11033	-0.41276	0.09198	C27	1.0756	0.22133	0.40618
C9	1.1061	-0.46271	0.13275	C28	1.09682	0.25927	0.54382
C10	1.09718	-0.48073	0.33622	C29	1.11626	0.24831	0.73563
C11	1.09098	-0.44885	0.49813	C30	1.11382	0.19952	0.7886
C12	1.09386	-0.39918	0.45656	C31	1.07268	-0.13971	0.0254
C13	1.1116	-0.10762	0.32218	C32	1.05634	-0.16881	-0.14936
C14	1.14428	-0.09516	0.49221	C33	1.00955	-0.16621	-0.23958
C15	1.1356	-0.05857	0.62899	C34	0.98059	-0.13432	-0.15551
C16	1.09497	-0.03501	0.5927	C35	0.99885	-0.10424	0.01696
C17	1.06033	-0.0515	0.4282	C36	1.04478	-0.10812	0.10462
C18	1.06998	-0.08752	0.2959	C37	0.9276	-0.13902	-0.21982
C19	1.09531	0.01327	0.6878	C38	0.91203	-0.09988	-0.31699
C39	0.86017	-0.10228	-0.34784	H88	1.17728	0.03979	0.66089

C40	0.82339	-0.14344	-0.27738	H89	1.05762	0.14333	0.35758
C41	0.83967	-0.18278	-0.18344	H90	1.06066	0.22907	0.25611
C42	0.89126	-0.18072	-0.15672	H91	1.13306	0.27705	0.84414
N43	0.76973	-0.14467	-0.29	H92	1.1291	0.19125	0.93716
C44	0.73621	-0.18777	-0.33982	H93	1.0782	-0.19377	-0.21
C45	0.68402	-0.19176	-0.32676	H94	0.99491	-0.19007	-0.36949
C46	0.66494	-0.15079	-0.27082	H95	0.97628	-0.08122	0.08859
C47	0.69992	-0.10621	-0.22897	H96	0.93981	-0.06731	-0.36457
C48	0.7521	-0.104	-0.23725	H97	0.84869	-0.07175	-0.4223
C49	1.19571	-0.16743	0.07447	H98	0.81231	-0.21436	-0.12297
C50	1.22956	-0.12296	0.03079	H99	0.90284	-0.21064	-0.07705
C51	1.27884	-0.12438	-0.03441	H100	0.74965	-0.2199	-0.3867
C52	1.29346	-0.16994	-0.05214	H101	0.65905	-0.2269	-0.36303
C53	1.25779	-0.21452	-0.01058	H102	0.68744	-0.07362	-0.18285
C54	1.20898	-0.21197	0.05034	H103	0.77818	-0.06987	-0.19414
C55	1.34673	-0.17032	-0.09963	H104	1.21867	-0.08821	0.05107
C56	1.37371	-0.19468	0.03548	H105	1.30613	-0.09009	-0.06317
C57	1.42494	-0.19281	0.00111	H106	1.26806	-0.24975	-0.02254
C58	1.45092	-0.16555	-0.18131	H107	1.35527	-0.214	0.17142
C59	1.42243	-0.14233	-0.31487	H108	1.44568	-0.21026	0.11108
C60	1.37121	-0.14432	-0.27316	H109	0.43981	-0.12256	-0.45139
N61	1.09479	0.4686	0.37956	H110	1.35018	-0.12564	-0.37735
C62	1.06173	0.41808	0.17361	H111	1.04552	0.43337	0.03593
C63	1.06015	0.33615	0.19867	H112	1.05414	0.37043	0.143
C64	1.09726	0.31011	0.49368	H113	1.13103	0.3584	0.88299
C65	1.11876	0.37103	0.73283	H114	1.12087	-0.58332	0.73859
C66	1.11826	0.45006	0.66276	H115	0.52055	-0.08624	-0.30206
N67	0.50434	-0.16227	-0.21619	H116	0.61149	-0.07883	-0.34001
C68	0.5356	-0.11851	-0.27512	H117	0.58992	-0.232	-0.16395
C69	0.58794	-0.11403	-0.2939	H118	1.49953	-0.23745	-0.13593
C70	0.60905	-0.15477	-0.25525	C119	0.64508	0.27276	1.14594
C71	0.57597	-0.19949	-0.19905	C120	0.6018	0.24016	1.22145
C72	0.52394	-0.20248	-0.18051	C121	0.60325	0.19032	1.24512
N73	1.11632	-0.13895	0.1519	C122	0.64754	0.17336	1.19305
N74	1.14552	-0.17432	0.15499	C123	0.69118	0.20772	1.1188
H75	1.05215	-0.23254	0.29982	C124	0.68879	0.25701	1.09832
H76	1.03728	-0.32351	0.33817	C125	0.64736	0.11989	1.20924
H77	1.18809	-0.31861	0.08908	C126	0.67146	0.09687	1.05605
H78	1.11843	-0.39896	-0.06498	C127	0.66958	0.04632	1.06674
H79	1.11114	-0.48702	0.00717	C128	0.64326	0.01768	1.22938
H80	1.08336	0.53751	0.65563	C129	0.61955	0.04037	1.38313
H81	1.08927	-0.37479	0.58289	C130	0.62184	0.09101	1.37379
H82	1.17665	-0.11151	0.5134	C131	0.61589	0.39933	1.14547
H83	1.16215	-0.04654	0.75568	C132	0.6434	0.42385	1.31373
H84	1.0297	-0.03371	0.39166	C133	0.64202	0.47346	1.34985
H85	1.01351	0.00029	0.72628	C134	0.61368	0.49824	1.21675
H86	1.01233	0.08799	0.73473	C135	0.58556	0.47179	1.05031
H87	1.17554	0.12665	0.67846	C136	0.58728	0.42281	1.0209
C137	0.6147	0.55166	1.24432	C186	0.03927	0.41548	0.53678

C138	0.57215	0.57046	1.19079	C187	0.12844	0.40726	0.38058
C139	0.57468	0.62109	1.19544	C188	0.15016	0.37453	0.27153
C140	0.61959	0.65448	1.25738	C189	0.11075	0.39009	0.40369
C141	0.66151	0.63572	1.31916	C190	0.04241	0.36988	0.52938
C142	0.65917	0.58499	1.31176	N191	0.6121	0.34939	1.0798
N143	0.62286	0.70705	1.2533	N192	0.65139	0.32423	1.10473
C144	0.6657	0.73844	1.17758	H193	0.56771	0.25263	1.25833
C145	0.66977	0.7893	1.17357	H194	0.56914	0.1647	1.29847
C146	0.62905	0.80912	1.24188	H195	0.72575	0.1965	1.07769
C147	0.58495	0.77599	1.31385	H196	0.69071	0.11765	0.92514
C148	0.58291	0.72551	1.32158	H197	0.68772	0.02921	0.94607
C149	0.57883	0.34454	0.9021	H198	0.59948	1.01882	1.51084
C150	0.55811	0.30196	0.78823	H199	0.60365	0.10763	1.4964
C151	0.51853	0.30316	0.6457	H200	0.66521	0.40524	1.41461
C152	0.50051	0.34673	0.61737	H201	0.66279	0.49227	1.48175
C153	0.52429	0.38986	0.72533	H202	0.56424	0.48902	0.94219
C154	0.56281	0.38741	0.86624	H203	0.53674	0.54601	1.14272
C155	0.45196	0.34587	0.50735	H204	0.54177	0.63424	1.14573
C156	0.44709	0.38497	0.37591	H205	0.69632	0.66035	1.37118
C157	0.39885	0.3901	0.3121	H206	0.69291	0.5723	1.35302
C158	0.35491	0.35646	0.38038	H207	0.6972	0.72443	1.11765
C159	0.35984	0.31592	0.5013	H208	0.70443	0.81269	1.1141
C160	0.40796	0.31046	0.56322	H209	0.5526	0.78897	1.37087
N161	0.3054	0.36587	0.34541	H210	0.54915	0.70138	1.38567
C162	0.28106	0.35366	0.1597	H211	0.5701	0.26802	0.81543
C163	0.23104	0.35873	0.13219	H212	0.50029	0.26964	0.56481
C164	0.20586	0.37718	0.29445	H213	0.51018	0.42313	0.71413
C165	0.23245	0.39115	0.48166	H214	0.48049	0.41273	0.33098
C166	0.28214	0.38499	0.5043	H215	0.39562	0.4216	0.21868
C167	0.70154	0.33865	1.01837	H216	0.32615	0.2898	0.55518
C168	0.72489	0.38421	0.93324	H217	0.41046	0.28042	0.66674
C169	0.77414	0.39023	0.85096	H218	0.29959	0.33836	0.03417
C170	0.79954	0.35105	0.85356	H219	0.21169	0.34678	-0.01325
C171	0.77477	0.30494	0.93806	H220	0.21486	0.40515	0.6123
C172	0.72558	0.29982	1.01742	H221	0.30154	0.39446	0.65168
C173	0.85099	0.35833	0.76028	H222	0.70573	0.41427	0.92862
C174	0.89197	0.34961	0.87813	H223	0.79265	0.42562	0.78522
C175	0.94113	0.35968	0.79424	H224	0.79288	0.27405	0.93684
C176	0.94919	0.37679	0.57426	H225	0.88609	0.33669	1.03761
C177	0.90742	0.3851	0.46371	H226	0.9725	0.35539	0.89238
C178	0.85919	0.37636	0.55519	H227	-0.08768	0.39893	0.30582
N179	0.63969	0.96541	1.23532	H228	0.82775	0.38378	0.46517
C180	0.59338	0.93357	1.21229	H229	0.55932	0.94739	1.19032
C181	0.5891	0.88266	1.21455	H230	0.55185	0.85869	1.19338
C182	0.63271	0.8636	1.23996	H231	0.71458	0.88484	1.29012
C183	0.67989	0.89725	1.26523	H232	0.7193	-0.02682	1.28248
C184	0.68257	0.94794	1.26233	H233	0.03102	0.44887	0.6176
N185	-0.00225	0.38461	0.46962	H234	0.16916	0.44747	0.36529
H235	0.06801	0.36349	0.48027	H236	1.02313	0.33474	0.65793

Table S3. Comparison of ReO_4^- detection limit of BTTA-BDNP with other materials

Methods	Probes	LOD	Ref.
Fluorescence	Auramine O	270 μM	1
	Thioflavin-T	260 μM	2
	TJNU-302	90 μM	3
	PMA	14 μM	4
	Ir-PAF	2.99 μM	5
	MOR-1	0.36 ppm	6
	MOR-2	0.15 ppm	7
	BTTA-BDNP	66.7 nM	This work

Table S4. Comparison of the reported adsorption for TcO_4^-/ReO_4^-.

Adsorbent	Target Anion	Capcity (mg/g)	Equilibrium time	Reference
TJNU-302	ReO_4^-	211	5 min	3
SLUG-21	ReO_4^-	602	>24 h	8
ZrO_2@rGO	ReO_4^-	43.55	5 h	9
4-ATR resin	ReO_4^-	354	8 h	10
PAF-1-F	ReO_4^-	420	250 min	11
SCU-100	ReO_4^-	541	30 min	12
SCU-101	ReO_4^-	217	10 min	13
SCU-102	ReO_4^-	291	20 min	14
SCU-103	ReO_4^-	318	5 min	15
$DhaTG_{Cl}$	ReO_4^-	437	30 min	16
3DCOF-g-$VBPPh_3Cl$	ReO_4^-	181	<1 min	17
BTTA-BDNP	ReO_4^-	648	2 min	This work

Table S5. Fitting results are based on the Langmuir and Freundlich models.

Isotherm model	Parameters
Langmuir	q_m = 726 mg g^{-1} K_L = 0.014 L mg^{-1} R^2 = 0.999
Freundlich	K_F = 182.91 (mg g^{-1})(L g^{-1})$^{4.56}$ n = 4.56 R^2 = 0.961

Table S6. Composition of simulated Hanford LAW melter recycle stream.

Anion	Concentration, mol/L	Anion: TcO_4^- molar ratio
TcO_4^-	1.94×10^{-4}	1.0
NO_3^-	6.07×10^{-2}	314
Cl^-	6.39×10^{-2}	330
NO_2^-	1.69×10^{-1}	873
SO_4^{2-}	6.64×10^{-6}	0.0343
CO_3^{2-}	4.30×10^{-5}	0.222

Table S7. Results of ReO_4^- sorption by TFPM-EP-Br from simulated Hanford waste.

Simulated wastes	Anions	Solid-to-liquid ratio (g/L)	Anion removal percentage (%)
Hanford waste	ReO_4^-	1:1	59.4%
	ReO_4^-	5:1	81.9%

REFERENCES

1 A. M. Desai, P. K. Singh, *Sens. Actuators B Chem.*, 2018, **277,** 205-209.

2 A. M. Desai, P. K. Singh, *Chem. Eur. J.*, 2019, **25,** 2035-2042.

3 C.-P. Li, H. Zhou, J. Chen, J.-J. Wang, M. Du, W. Zhou, *ACS Appl. Mater. Interfaces,* 2020, **12,** 15246-15254.

4 G. Singh, S. P. Pandey, P. K. Singh, *Sens. Actuators B Chem.*, 2021, **330,** 129346.

5 D. Xu, L. Chen, X. Dai, B. Li, Y. Wang, W. Liu, J. Li, Y. Tao, Y. Wang, Y. Liu, G. Peng, R. Zhou, Z. Chai, S. Wang, *ACS Appl. Mater. Interfaces*, 2020, **12,** 15288-15297.

6 S. Rapti, S. A. Diamantis, A. Dafnomili, A. Pournara, E. Skliri, G. S. Armatas, A. C. Tsipis, I. Spanopoulos, C. D. Malliakas, M. G. Kanatzidis, J. C. Plakatouras, F. Noli, T. Lazarides, M. J. Manos, *J. Mater. Chem. A.*, 2018, **6,** 20813-20821.

7 V. Amendola, G. Bergamaschi, M. Boiocchi, R. Alberto, H. Braband, *Chem. Sci.*, 2014, **5,** 1820-1826.

8 H. Fei, M. R. Bresler, S. R. J. Oliver, *J. Am. Chem. Soc.*, 2011, **133,** 11110-11113.

9 Y. Gao, K. Chen, X. Tan, X. Wang, A. Alsaedi, T. Hayat, C. Chen, *ACS Sustain. Chem. Eng.*, 2017, **5,** 2163-2171.

10 C. Xiong, C. Yao, X. Wu, *Hydrometallurgy*, 2008, **90,** 221-226.

11 D. Banerjee, S. K. Elsaidi, B. Aguila, B. Li, D. Kim, M. J. Schweiger, A. A. Kruger, C. J. Doonan, S. Ma, P. K. Thallapally, *Chem. Eur. J.*, 2016, **22,** 17581-17584.

12 D. Sheng, L. Zhu, C. Xu, C. Xiao, Y. Wang, Y. Wang, L. Chen, J. Diwu, J. Chen, Z. Chai, T. E. Albrecht-Schmitt, S. *Wang, Environ. Sci. Technol.*, 2017, **51,** 3471-3479.

13 L. Zhu, D. Sheng, C. Xu, X. Dai, M. A. Silver, J. Li, P. Li, Y. Wang, Y. Wang, L. Chen, C. Xiao, J. Chen, R. Zhou, C. Zhang, O. K. Farha, Z. Chai, T. E. Albrecht-Schmitt, S. Wang, *J. Am. Chem. Soc.*, 2017, **139,** 14873-14876.

14 D. Sheng, L. Zhu, X. Dai, C. Xu, P. Li, C. I. Pearce, C. Xiao, J. Chen, R. Zhou, T. Duan, O. K. Farha, Z. Chai, S. Wang, *Angew. Chem. Int. Ed.,* 2019, **58,** 4968-4972.

15 N. Shen, Z. Yang, S. Liu, X. Dai, C. Xiao, K. Taylor-Pashow, D. Li, C. Yang, J. Li, Y. Zhang, M. Zhang, R. Zhou, Z. Chai, S. Wang, *Nat. Commun.*, 2020, **11,** 5571.

16 H.-J. Da, C.-X. Yang, X.-P. Yan, *Environ. Sci. Technol.*, 2019, **53,** 5212-5220.

17 Y. Wang, J. Lan, X. Yang, S. Zhong, L. Yuan, J. Li, J. Peng, Z. Chai, J. K. Gibson, M. Zhai, W. Shi, *Adv. Funct. Mater.*, 2022, **32,** 2205222.